Materials Research Proceedings **27** (2023) 357-364 https://doi.org/10.21741/9781644902455-46

Comparative strain survey of an aerospace structure using distributed fibre optic strain sensing technology

Gerard Natividad[1, a *], Suzana Turk[1,b], Kelly Tsoi[1,c] and Daniel Bitton[1,d]

[1]506 Lorimer Street, Fishermans Bend 3207 VIC, Australia

[a]gerard.natividad@defence.gov.au, [b]suzana.turk@defence.gov.au, [c]kelly.tsoi@defence.gov.au, [d]daniel.bitton@defence.gov.au

Keywords: Fibre Optic Sensor (FOS), Distributed Strain Sensing, Structural Health Monitoring (SHM)

Abstract. Significant strides have been made in non-proprietary distributed FOS technologies suitable for structural health monitoring (SHM) applications. FOSs are resistant to electromagnetic interference, corrosion, and high-strain cyclic loading while also providing significant reductions in weight and the complexity of installation when compared to conventional electrical resistance foil strain gauges (FSGs). This paper builds on previous benchmarking of proprietary distributed FOSs and demonstrates a FOS-based high-density strain measurement capability on a large aircraft structure subjected to representative flight loading.

Introduction

The structural assessment and health monitoring of aerospace structures is customarily undertaken using experimental measurements of strain obtained from conventional FSGs. Strain predictions in fatigue-critical locations are obtained using analytical and computational modelling and are experimentally verified using measurements from FSGs installed at these locations. While FSGs provide an effective means of measuring strain at single locations, they are not well suited to determining the location of peak strain. Additionally, FSGs provide strain measurements averaged over the gauge length. This can lead to uncertain strain measurements at high strain gradient locations because a small shift in the FSG installation position can lead to a significant change in measured strain value. Strain monitoring using FSGs can be inconvenient due to the volume of associated wiring, and cable management and connectivity requirements. FSGs also involve a high maintenance burden, in part because of their susceptibility to fatigue. The need for gauge re-calibration, repair or replacement is not uncommon in large installations.

Distributed FOS technology presents an opportunity to improve the reliability and spatial resolution of airframe strain sensing, while also significantly reducing the installation and maintenance burden. In combination with FEA, distributed FOSs have the potential to provide an improved basis for identifying the magnitude and location of peak strain and high strain gradients in fracture critical structures.

This paper reports on the performance of distributed FOSs for the purpose of structural assessment of an aircraft structure. Performance factors including sensor durability and measurement accuracy are quantified and compared to FSGs. An adhesive packaging technique for FOS installation is also assessed for robustness and strain transfer effectiveness compared to FSGs.

Materials Research Proceedings **27** (2023) 357-364 https://doi.org/10.21741/9781644902455-46

Experimental Method

The present work uses a distributed FOS capability based on All Grating Fibre (AGF) technology [1] and the Sensuron Summit Optical Frequency Domain Reflectometry (OFDR) interrogation system. A 3.25 m long AGF sensor with 2024 sensing points was selected to provide strain measurements every 1.6 mm with a notional strain measurement accuracy of ±1με. This type of FOS is mechanically robust with a 5% ($50{,}000\ \mu\epsilon$) tensile failure strain [1] and exceptional fatigue resistance [2].

FOSs were installed on a geometrically complex airframe structure undergoing full-scale fatigue testing. These sensors were bonded to known fracture critical structural members, as well as other areas important to the structural integrity of the fatigue test article. FOSs were installed adjacent and parallel to 15 EA-series self-compensating FSGs [3] to enable direct comparison of strain readings at multiple locations throughout the structure.

A high-strain fatigue resistant packaging and adhesive strategy described in [4] was used for the installation of the FOSs. The FOSs are adhered using LOCTITE EA9309.3NA two-part epoxy which has excellent peel strength and elongation properties, and can withstand harsh environments. Airtech tac-strip adhesive mesh tape was used to position and immobilise FOSs, control bondline thickness and provide protection from mechanical damage.

The key steps in the installation method are depicted in Fig. 1. Bridging sleeves were installed along the installation path to protect unbonded sections of fibre. The fibre was threaded through the bridging sleeves, temporarily secured in position using masking tape and immobilised using the adhesive mesh tape. Adhesive was applied on top of the mesh tape and smoothed thoroughly across the mesh cells to encapsulate the FOS and remove excess adhesive. The adhesive partially cures and is solid to touch within 12 hours and is fully cured in 3-5 days at room temperature.

A baseline zero-load state was recorded for the installed FSGs and FOSs. All subsequent strain measurements are relative to this baseline. That is, changes in strain resulting from load application to the structure were measured from this original undisturbed condition.

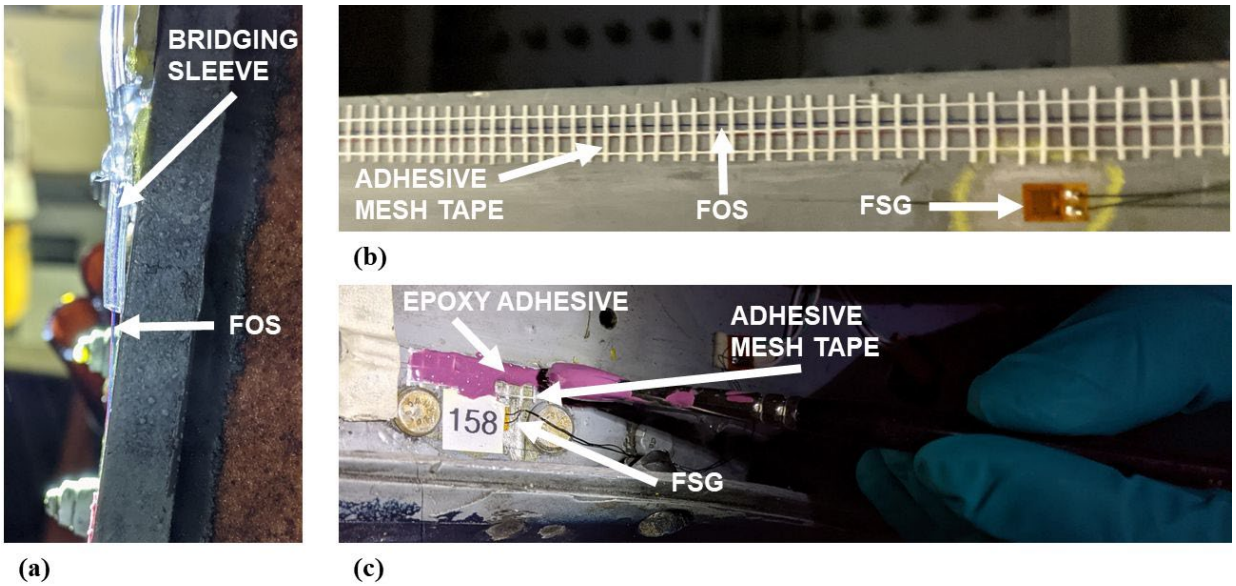

Fig. 1 FOS installation method: (a) FOS inserted through bridging sleeves, (b) mesh tape is adhered on top of FOS, and (c) a fine paintbrush is used to encapsulate the FOS and mesh tape in epoxy adhesive

Results

As part of the full-scale fatigue testing of this airframe structure, strain surveys were conducted before and after a sequence of flight representative variable amplitude loading, to establish an initial strain correlation between the FOSs and FSGs and repeatability of the measurements. The present work reports on the strain survey results on a flange at a fracture-critical location on the structure shown in Fig. 2. The graph shows the FOS strain distribution at peak load and is aligned with a photo of the structure showing the position of structural features in relation to the strain distribution. For example, the three stiffeners intersecting the flange in the photo are represented by black solid lines on the graph and correspond to local increases in strain.

The position of two FSGs are labelled in Fig. 2 and the corresponding strain values show excellent agreement with values obtained from the fibre. It is to be noted that the strain values obtained from FSGs alone provide no indication of the strain gradient nor of the peak strain locations in the structure, both of which are provided by the FOS. In this case, the peak strain obtained from the FOS occurred at the stiffener adjacent to FSG1. This peak strain is ~26% higher than the FSG1 strain value.

Fig. 3 shows the strain distribution in a flange at a different location. The FSG strain value here shows excellent agreement with the corresponding fibre measurement, however the strain gradient at this location is more severe than in the previous location. According to the FOS, the strain at the FSG location ranges between 1191-1402 με across the 5 mm gauge length so a minor shift in FSG position would significantly alter the strain reading. Since the distributed FOS averages strain across a shorter 1.6 mm gauge length, it is more suitable for high strain-gradient measurement situations such as this.

Periodic small-amplitude perturbations were observed in some of the strain distribution profiles, evident for example in the profile to the left of the FSG1 location in Fig 2. These perturbations manifested in consistent locations and maintained the same amplitude across different strain surveys. Similar features were observed in strain profiles published in the open literature although no hypotheses were provided on possible causes. A coupon test was conducted to investigate the cause. This indicated a combination of systematic noise from the interrogator, which appeared to increase with applied strain, and the effect of the mesh tape impinging on the FOSs under applied load, as the most likely causes. Nevertheless, the perturbations are negligible in magnitude compared to the strain peaks caused by structural features such as stiffeners, e.g. the peak strain corresponding to the stiffener adjacent to FSG1 in Fig. 2. Therefore, the overall FOS strain distribution and magnitudes were considered reliable.

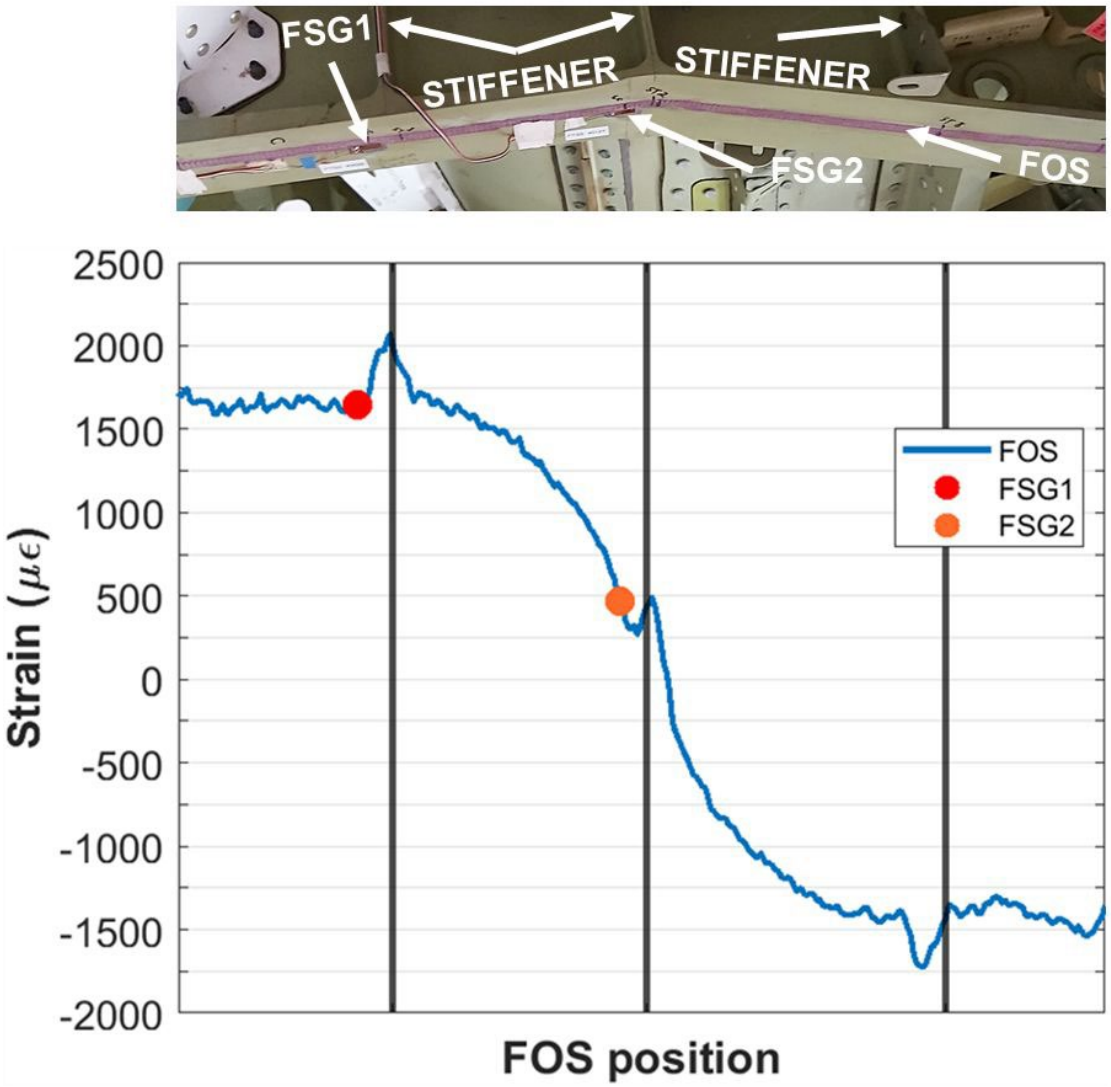

Fig. 2 Line graph showing strain profile obtained from FOS in a flange with three stiffener intersections (labelled in photo and represented by black solid lines in graph) and two FSGs (labelled and represented by markers on line graph)

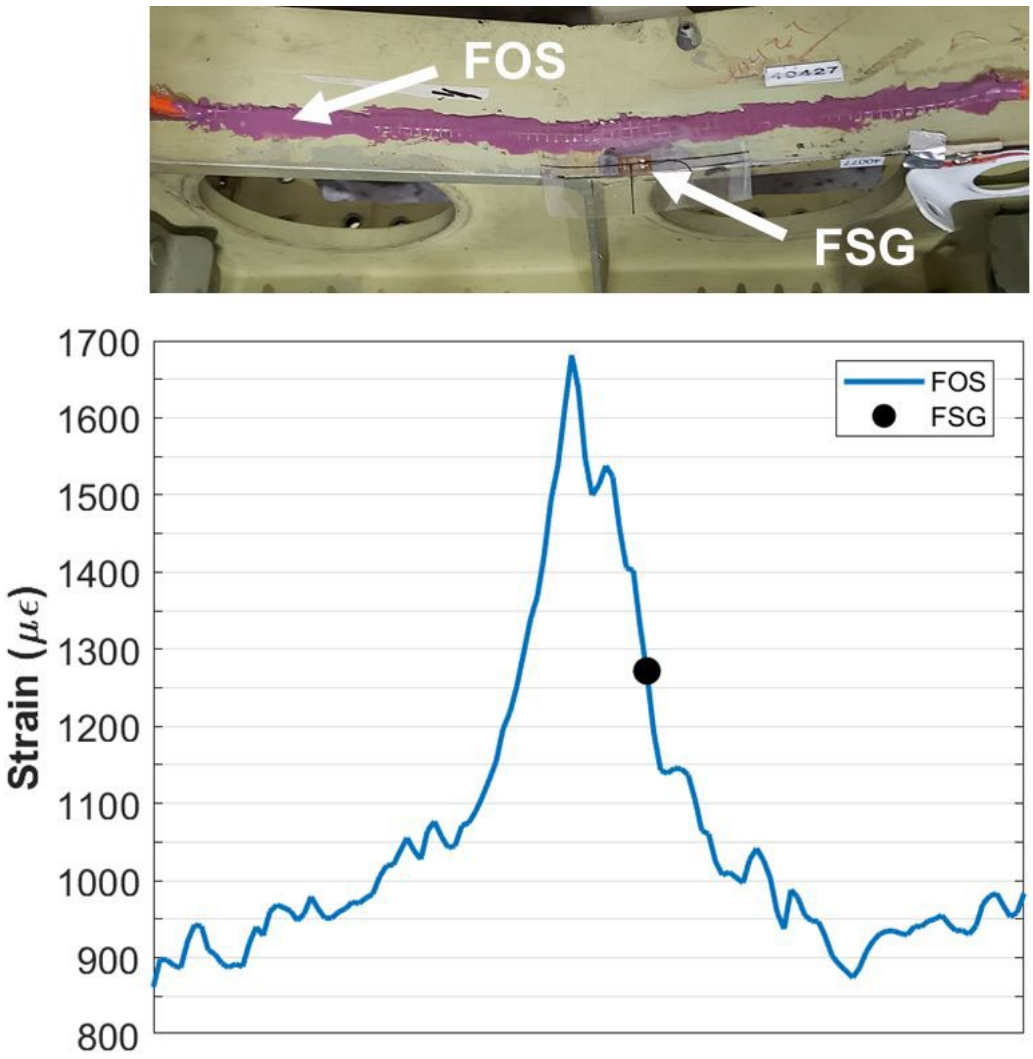

Fig. 3 Strain profile obtained from FOS on a flange showing FSG position in a high strain gradient location

Fig. 4a and Fig. 5a show strain comparisons between readings from FSG1 and FSG2 and corresponding FOS values (refer to Fig. 2), recorded continuously during a strain survey load application sequence. FSG data was recorded at a sampling rate of 10 Hz and FOS data at 16 Hz. The FSG and FOS strain values are in close agreement at all applied loads, as shown by the overlapping line graphs. Fig. 4b and Fig. 5b show the comparative strain response during a 15-second interval at peak strain. The difference between the FOS and FSG1 measured strains was approximately 45 μƐ at a peak strain of 1650 μƐ, Fig. 4b. As the FOS and FSG sensors are not coincident, a small difference in measured strain values is not unexpected. The noise level for this FOS system (comprising sensor and interrogator) at an acquisition rate of 16 Hz is approximately 5 μƐ which is 0.3 % of the strain at this load level. The difference between FOS and FSG2 measured strains was approximately 10 μƐ at a peak strain of 465 μƐ (Fig. 5b).

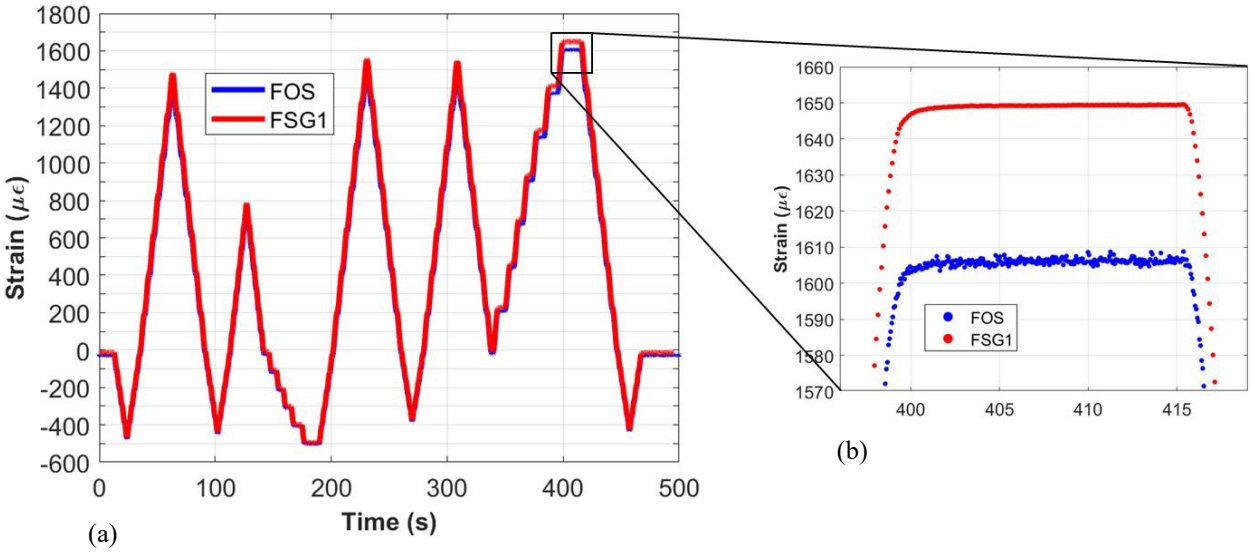

Fig. 4 FOS and FSG1 (refer to Fig. 2) strain response during (a) the strain survey load sequence and (b) FOS and FSG1 strain response during a 15 second interval at peak strain

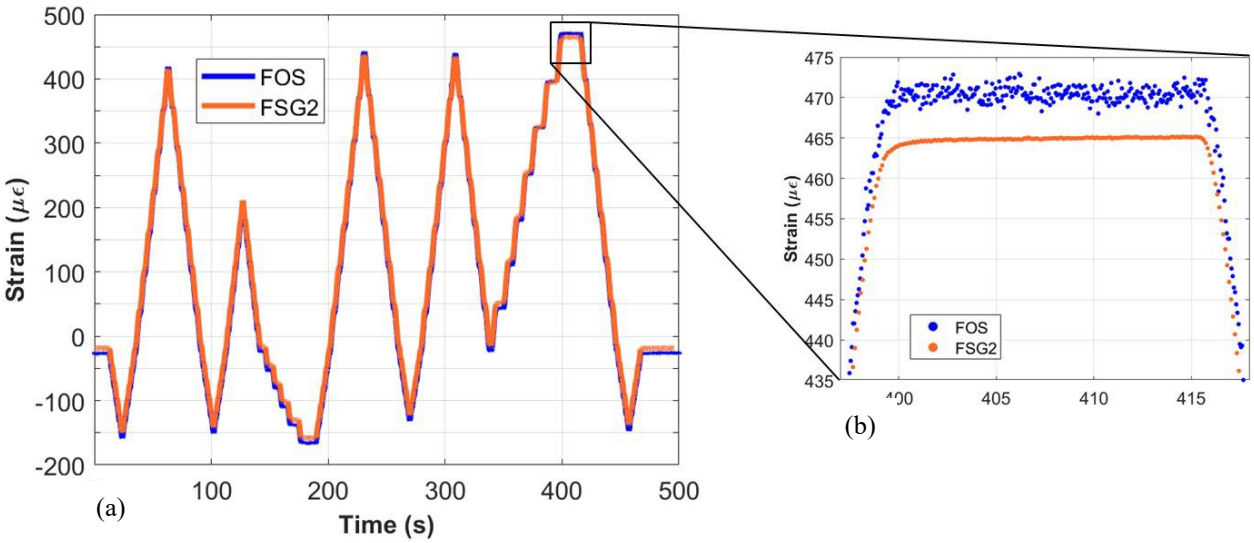

Fig. 5 FOS and FSG2 (refer to Fig. 2) strain response during (a) the strain survey load sequence and (b) FOS and FSG2 strain response during a 15 second interval at peak strain (right)

Strain surveys were conducted routinely during the full-scale fatigue test to monitor FSG strain-drift. Strain values were compared across multiple strain surveys at the two FSG locations shown in Fig. 2. Measured strain remained consistent between the first and last strain survey, the latter conducted following one lifetime of simulated flying hours. However, FSG strain-drift was observed at other locations. FSGs are capable of measuring maximum elongations in the range 3 % - 5 % [5,6] but are subject to fatigue damage - the fatigue life of EA-series FSGs is approximately 10^6 cycles at ± 1500 με [7]. FOSs do not experience strain drift or fatigue damage under normal operating conditions, as specified in [1]. Previous testing by the authors showed that draw tower gratings, which are similar to AGF, survived an incremental constant amplitude loading sequence (Table 1) accumulating 3 million applied load cycles, with failure eventually occurring at a strain of 23,000 με [2].

Table 1 Incremental loading sequence for FOS fatigue test

Peak Strain (με)	10,000	15,000	17,000	19,000	21,000	23,000	25,000
Load Cycles (million)	1	0.5	0.5	0.5	0.5	0.5	0.5

It was previously mentioned that FOSs provide significant reductions in weight and complexity of installation relative to FSGs. Fig. 6a compares the electrical wiring and cable management corresponding to 88 FSGs installed on the aircraft structure, to 4 yellow-jacketed FOS cables accommodating 3300 sensors, Fig. 6b. This comparison highlights how distributed FOS enables high-density strain measurement across a large area of structure to be achieved with a relatively low sensor footprint.

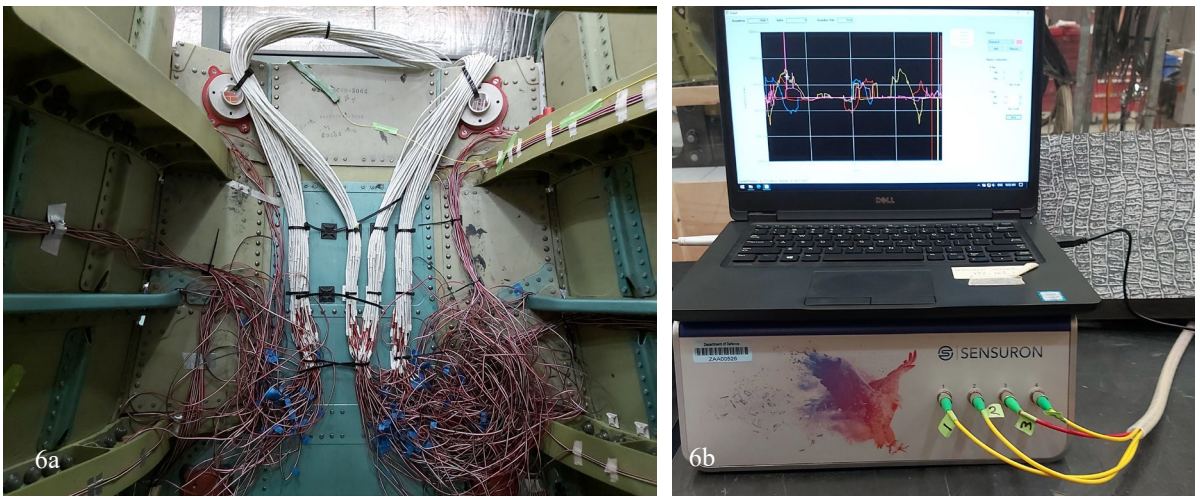

Fig. 6 Wiring and cable management for 88 FSGs (Fig. 6a), and yellow-jacketed FOS cables accommodating approximately 3300 sensors (Fig. 6b). FOS cables are shown connected to the 4-channel Sensuron Summit interrogator and laptop showing live strain distribution during applied loading

Conclusions

This paper evaluated the performance of an FOS-based high-density strain measurement capability on an aircraft structure. The structure was subjected to applied loads in a strain survey before and after one lifetime of simulated flying hours. The comparative evaluation focused on strain values obtained from FOSs installed directly adjacent to 2 of the 15 FSGs that were considered representative of all 15 FSGs.

The measured strain values obtained from corresponding FOSs and FSGs showed excellent agreement. The high-density distributed FOS strain measurements provided information about the magnitude and location of peak strain and high strain gradients that is unavailable from FSGs. Additionally, the comparative strains were consistent in multiple strain surveys thus demonstrating a good level of repeatability and reliability of the FOS technology.

The adhered FOSs are mechanically robust, withstanding for the moment one lifetime of simulated flying hours (6000 FH of a combat aircraft) and strains up to 4000 με and are still working. The adhesive packaging technique provided sufficient protection to the fibres whilst maintaining adequate strain transfer between the host structure and FOS.

Perturbations were present on all strain profiles, which appear to be a result of low-amplitude systematic noise. However, these perturbations were negligible compared to the magnitude of

strain peaks caused by structural elements such as stiffeners. Therefore, the overall FOS strain distribution was considered reliable.

The results presented in this paper demonstrate some key advantages of distributed FOSs for airframe strain monitoring applications, including reliable and repeatable high-density strain measurements and a relatively small sensor footprint.

Acknowledgements
The authors acknowledge the Structures and Materials Test Centre facility at DSTG and the technical assistance of Isaac Field and Keith Muller. The authors also acknowledge the collaborative opportunity provided by RMIT University, RUAG International and Armasuisse.

References

[1] Information on https://fbgs.com/components/all-grating-fibers-agf/

[2] N. Zhang, C. Davis, W.K. Chiu, T. Boilard & M. Bernier, Fatigue performance of Type I fibre Bragg grating strain sensors. Sensors 2019, 19, 3524. https://doi.org/10.3390/s19163524

[3] Micro-Measurements, Gage series – stress analysis gages. Technical data sheet, Document No. 11506, 30/05/2018.

[4] N. Zhang, S. Turk, D. Bitton, C. Davis and W.K. Chiu, A review of high strain fatigue resistant packaging and adhesives for use with fibre optic sensors. DST-Group-TN-2235, Commonwealth of Australia, 2022.

[5] Micro-Measurements, Strain gauge selection criteria, procedures, recommendations, Tech Note TN-505, 01/11/2010.

[6] Micro-Measurements, High elongation strain measurements, Tech Tip TT-605, 13/07/2015.

[7] Micro-Measurements, Fatigue characteristics of Micro-Measurements strain gages, Tech Note TN-508-1, 01/11/2010.